

# NAVAL POSTGRADUATE SCHOOL MONTEREY, CALIFORNIA



## THESIS

**DESIGN AND EVALUATION OF MINE AND UXO  
DETECTORS FOR AUTONOMOUS MOBILE  
ROBOTS**

by

Curtis J. Goodnight

September, 1996

Thesis Advisor  
Thesis Co-Advisor

Xiaoping Yun  
David Cleary

19970121 202

Approved for public release; distribution is unlimited.

# REPORT DOCUMENTATION PAGE

Form Approved OMB No. 0704-0188

Public reporting burden for this collection of information is estimated to average 1 hour per response, including the time for reviewing instruction, searching existing data sources, gathering and maintaining the data needed, and completing and reviewing the collection of information. Send comments regarding this burden estimate or any other aspect of this collection of information, including suggestions for reducing this burden, to Washington Headquarters Services, Directorate for Information Operations and Reports, 1215 Jefferson Davis Highway, Suite 1204, Arlington, VA 22202-4302, and to the Office of Management and Budget, Paperwork Reduction Project (0704-0188) Washington DC 20503.

1. AGENCY USE ONLY <i>(Leave blank)</i>	2. REPORT DATE <b>September 1996.</b>	3. REPORT TYPE AND DATES COVERED  <b>Master's Thesis</b>	
4. TITLE AND SUBTITLE <b>DESIGN AND EVALUATION OF MINE AND UXO DETECTORS FOR AUTONOMOUS MOBILE ROBOTS</b>		5. FUNDING NUMBERS	
6. AUTHOR(S) <b>Curtis J. Goodnight</b>		8. PERFORMING ORGANIZATION REPORT NUMBER	
7. PERFORMING ORGANIZATION NAME(S) AND ADDRESS(ES) <b>Naval Postgraduate School Monterey CA 93943-5000</b>		10. SPONSORING/MONITORING AGENCY REPORT NUMBER	
9. SPONSORING/MONITORING AGENCY NAME(S) AND ADDRESS(ES)		11. SUPPLEMENTARY NOTES <b>The views expressed in this thesis are those of the author and do not reflect the official policy or position of the Department of Defense or the U.S. Government.</b>	
12a. DISTRIBUTION/AVAILABILITY STATEMENT <b>Approved for public release; distribution is unlimited.</b>		12b. DISTRIBUTION CODE	
13. ABSTRACT <i>(maximum 200 words)</i>  <b>This study focuses on the development of a light weight metal detector to be used for the purpose of mine / Unexploded Ordnance (UXO) detection. The detector was developed based upon a twin oscillator design, and the performance of this design was tested with respect to diameter of the sensing coil, operating frequency, and the number of turns of the sensing coil. The results of this study provide a field tunable, light weight, low power mine / UXO detector with significant range. The ability to equip a robot with this device and send it into the field will prove to be an invaluable asset to ongoing mine sweeping operations.</b>			
14. SUBJECT TERMS <b>MINE DETECTOR, UNEXPLODED ORDNANCE, TWIN OSCILLATOR</b>		15. NUMBER OF PAGES <b>66</b>	
17. SECURITY CLASSIFICATION OF REPORT <b>Unclassified</b>		16. PRICE CODE	
18. SECURITY CLASSIFICATION OF THIS PAGE <b>Unclassified</b>	19. SECURITY CLASSIFICATION OF ABSTRACT <b>Unclassified</b>	20. LIMITATION OF ABSTRACT <b>UL</b>	



Approved for public release; distribution is unlimited.

**DESIGN AND EVALUATION OF MINE AND UXO DETECTORS FOR  
AUTONOMOUS MOBILE ROBOTS**

Curtis J. Goodnight  
Lieutenant, United States Navy  
B.S., Naval Postgraduate School, 1996

Submitted in partial fulfillment  
of the requirements for the degree of

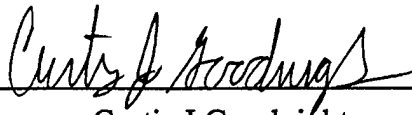
**MASTER OF SCIENCE IN ELECTRICAL ENGINEERING**

from the

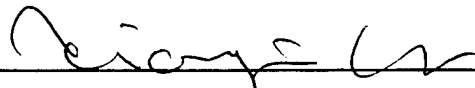
**NAVAL POSTGRADUATE SCHOOL**

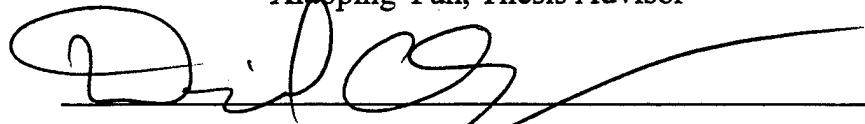
**September 1996**

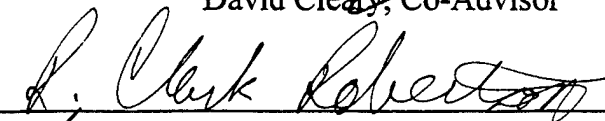
Author:

  
Curtis J Goodnight

Approved by:

  
Xiaoping Yun, Thesis Advisor

  
David Cleary, Co-Advisor

  
for Herschel H Loomis, Jr., Chairman,  
Department of Electrical and Computer Engineering



## ABSTRACT

This study focuses on the development of a light weight metal detector to be used on small autonomous robots for the purpose of mine / Unexploded Ordnance (UXO) detection. The detector was developed based upon a twin oscillator design, and the performance of this design was tested with respect to diameter of the sensing coil, operating frequency, and the number of turns of the sensing coil. The results of this study provide a field tunable, light weight, low power mine / UXO detector with significant range. The ability to equip a robot with this device and send it into the field will prove to be an invaluable asset to ongoing mine sweeping operations.



## TABLE OF CONTENTS

<b>I. INTRODUCTION</b> .....	1
A. BACKGROUND.....	1
B. PROBLEM STATEMENT.....	4
C. ASSUMPTIONS.....	5
D. THEORY / LITERATURE REVIEW.....	6
1. Twin Oscillators.....	6
2. Oscillators.....	9
3. Filters.....	10
4. Digital Logic.....	13
<b>II. DESCRIPTION OF SENSOR</b> .....	19
A. PRINCIPLE.....	19
B. IMPLEMENTATION.....	21
1. Power.....	21
2. Frequency Reference Side.....	23
3. Sensor Side.....	25
4. Output Signal Circuitry.....	30
5. Frequency Division.....	32
<b>III. TESTING / RESULTS</b> .....	37
A. TESTING.....	37
B. RESULTS.....	39
1. Data Obtained.....	39
2. Data Discrepancies.....	44
3. Conclusions.....	48
<b>IV. DISCUSSION</b> .....	51
A. APPLICATION.....	51
B. FUTURE WORK.....	51

LIST OF REFERENCES.....	53
INITIAL DISTRIBUTION LIST.....	55

## ACKNOWLEDGMENTS

Several people have contributed to the completion of this thesis. I would, however, like to specially thank my two thesis advisors who have exercised much patience and understanding through many problems encountered along the way. Dr. Xiaoping Yun and Dr. Dave Cleary deserve all the credit in the world for sticking with me during this project. Thank you for your support and guidance.

I would also like to acknowledge the man who quite literally was my left arm during the building phase of this project. Due to serious injury, I lost the use of my left arm and hand. Warren Rogers volunteered to assemble anything I designed. I'm not sure he knew what he was getting into, but he spent much time rebuilding my "brilliant ideas." His selfless devotion deserves great recognition for the completion of this thesis. Again, my sincerest thanks.

## I. INTRODUCTION

### A. BACKGROUND

"An estimated 100 million or more of these indiscriminate killers have been deployed worldwide, maiming or killing 26,000 people a year." [Ref. 1: p. 62] These indiscriminate killers are land mines. Land mines and unexploded ordnance left in the ground after a regional conflict are not a trivial problem in the international community. In some countries, land mines are an extreme problem. Cambodia has so many unexploded mines that half of the country cannot be inhabited. Kuwait was forced to extract seven million mines scattered in the countryside as a result of Desert Storm. From 1992 to 1995, U.N. peace keepers have reported 20 deaths and over 100 incidents related to mines.

Land mines in Bosnia represent the current threat to United States troops. In Bosnia alone there are as many as 5,000,000 mines of 2,500 different varieties. While Swedish peace keepers are using fairly sensitive metal detectors, the US Army is still utilizing Korean -War vintage technology in their mine sweeping operations. The mine sweeping technology currently being used in Bosnia includes the use of a titanium probe to stick in the ground and look for buried mines. The probe has a special tip so as not to activate magnetic mines. As for contact mines, the titanium probe is not the optimal tool.

The problem facing the world is to detect plastic and metal cased mines and to be able to distinguish them from background clutter. With the notable

exception of biological and chemical land mines, most mines can be easily disarmed after detection. Science is beginning to tackle the most important stage in mine disarmament, detection. The work in the area of detection is heading in different directions, with the consensus that no one type of sensor is the answer to the problem, but rather, a fusion of sensors is required to obtain a complete picture.

Man-portable mine detectors are one category of sensor. The Austrian built AN/PSS-12 pulse -induction metallic mine detector is the primary land mine hunting device in use. In 1995, advanced hand held detectors were demonstrated that would help in the hunt for plastic and other non metallic mines. There are four of these advanced detectors being evaluated. Three of these advanced detectors are ground penetrating radars, and one is an infrared detector. These four detectors have gone past the prototype stage and are in formal development. . The obvious disadvantage to this approach is that a human operator is needed, and this is inherently dangerous.

Other categories of sensors include ground vehicle detectors, airborne detectors, sound detectors, and X-ray backscatter detectors. The ground vehicle detectors are likely to employ all of the above types of sensors (FLIR cameras, GPR, and pulse induction metal detectors). All of these sensors would then be mounted upon a blast hardened vehicle. The Army is currently developing ASTAMIDS, the Airborne Standoff Minefield Detection System. This system will be deployed on the Hunter UAV (airborne) surveillance

platform. It uses passive infrared to detect the size of an object. The problem with this sensor is that rocks and land mines of the same size are not distinguishable from each other.

The use of sound detectors is still in preliminary phases, and the results are not very promising. The sound detection is only capable of resolving objects of at least 5 centimeters of length at a distance of 6 centimeters. Other limitations are the need for the scan to hit the target directly to find its shape, and the limitation of a slow scan rate that makes this process time consuming.

X-ray backscatter is a promising technology. Originally the process used two different X-rays, each having a different energy. The two X-rays would be compared, and the surface return would be subtracted out by comparing the two pictures. This worked well, but in order to obtain any distance, enormous energy was required. A new sensor using just one X-ray source was developed that works on the principle that photon absorption of mines is less than soil, and it therefore scatters more photons. This scattering can be used to image the land mine. The X-ray backscattering systems can show the shape of the mine and approximate its depth down to about 4 inches.

The purpose of this thesis is to investigate the parameters of a metal detection device so that it may be mounted upon a small autonomous robot. This would open the possibility of allowing robots to perform the function of land mine detection. The immediate advantage is that unlike the man portable mine detectors, the risk to human life is considerably diminished, if not eliminated in

its entirety. Another advantage is that machines do not require rest and are better suited to the tedium and exactness required to sweep a minefield. The ultimate vision is to incorporate this metal detection device with all of the sensor types mentioned above, and perhaps some new technology, into a cohesive, robotic "small unit operations" role. When the need for mine sweeping exists, a team arrives with its computer controlled robots, inputs the parameters of the search, and collects the data for further use/detonation.

It appears that the Army is well on its way to providing automated sensing with the use of the ASTAMIDS system that was described above. This thesis will center upon the metal detecting portion of mine detection. The reason for this decision is the fact that in a recent U.N. conference in Geneva, it was agreed upon that all anti-personnel land mines are to be detectable (i.e. made at least partly of metal) and have a limited life span. The ASTAMIDS system and a robust metal detection system working together could be a useful tool, and a huge step towards realizing an automated mine detection unit.

## **B. PROBLEM STATEMENT**

The problem at hand is to design a detector to function as a metal detector that is small enough and sensitive enough to be placed upon an autonomous robot. This robot would then be used to sweep minefields instead of risking the safety of personnel.

As stated above, the overall purpose of this thesis is to design a metal detector. It is true that metal detectors already exist in the field today, but the problem with integrating these particular devices onto an autonomous platform is that they are intended for use by a soldier, and give an audible tone to denote detection, and, more importantly come in predetermined, rigid shapes and sizes whose physical characteristics cannot be easily changed. This thesis will provide a baseline of data for the designer of an overall mine detection system to choose the components of a metal detector that will suit his particular size and range requirements. From the graphs provided in this thesis, the designer will be able to attain the appropriate coil size required for a sensor and the appropriate frequency at which to run the metal detection circuit in order to achieve a specified range of detection for a specific sized target.

### **C. ASSUMPTIONS**

Due to the fact that this product is to be used upon a mobile robot, assumptions were made as to the approximate size of the coil, and the probable power supply voltage. The numbers decided upon were to make the inductor coil no greater than 12 inches in diameter, and a minimum diameter of no less than four inches. The power supply was chosen to be between 15 and 5 volts positive, and a matching negative power supply must be available. The number of turns was arbitrarily chosen to be less than 100, because exceeding this number makes the inductor bulky. Also, the shielding that may be required to

electromagnetically isolate the sensor from an actual robot upon which it may be mounted was not taken into consideration due to the difficulty of predicting the geometry of mounting, or the radiative parameters of any particular robot.

## **D. THEORY / LITERATURE REVIEW**

### **1. Twin Oscillators**

The most critical piece of literature reviewed was the schematic of the twin oscillator from Reference 3. Shown in Figure 1.1 on the next page, this oscillator forms the basis of my attempts to create a small, sensitive metal detector. This detector utilizes the C-MOS 4030 chip to provide the functions of an amplifier and an exclusive-or gate. The 4030 chip is designed for the function of exclusive-or, but the logic also provides a 5 volt high output, and it provides a 0 volt low output, thus providing amplification to potentially weak signals. Each gate supplies the next gate with sufficient power.

Starting with gate A1, a coil and a capacitor are attached to one input of the executive-or gate. This will create a natural frequency. This natural frequency is given by the formula:

$$\omega^2 = 1 / LC$$

where L is the inductance provided by the coil, and C is the capacitance of the capacitor in the 100 pF position of Figure 1.1.

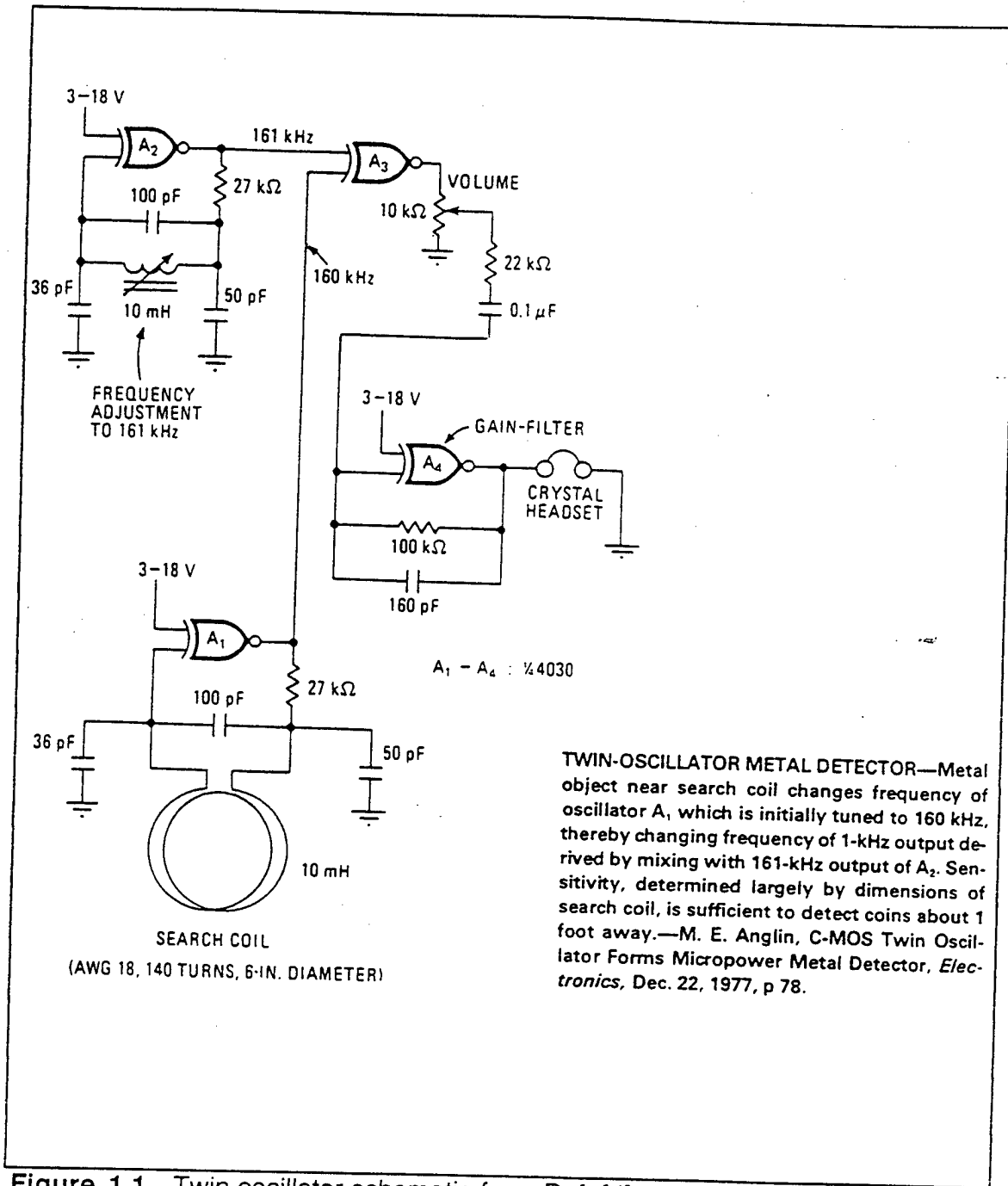


Figure 1.1 Twin oscillator schematic from Ref. [4]

The exclusive-or gate labeled A2 has its frequency controlled exactly the same way, except that a tunable inductance coil is utilized to attain a frequency that is exactly 1 kHz greater than the output of exclusive-or gate A1.

The outputs from exclusive-or gate A1 and exclusive-or gate A2 are sent through exclusive-or gate A3, where an output of the sum of the two input frequencies and the difference between the two output frequencies is generated and sent to the rest of the circuit. (The explanation of the exclusive-or gate as a mixer is given below in this section). Gain control for the volume of the difference is the function of exclusive-or gate A4. The result of this model circuit is an audible tone that is the frequency difference between the A2 gate output and the A1 gate output. The sum frequency from the A3 exclusive-or gate is filtered out by the frequency response of one's ears. The key to the circuit is that as metal is placed near the search coil that inputs to gate A1, the overall inductance (L) of the coil as seen by the circuit goes up. As can be seen from the above equation, inductance and frequency share an inverse relationship. As inductance increases, the resulting frequency will decrease. This occurrence will create a larger difference between the outputs of exclusive-or gates A1 and A2. This in turn will increase the frequency of the audible signal heard at the output.

## 2. Oscillators

Obviously, in a twin oscillator device, the construction of oscillators is of extreme importance. Sedra and Smith, in Reference 5, discuss several different oscillators, and give guidance for their use and limitations. The practical oscillator of interest which incorporates op amps and RC networks is the Wien-bridge oscillator. Figure 1.2 provides a component diagram of an oscillator that was originally implemented into the working circuit.

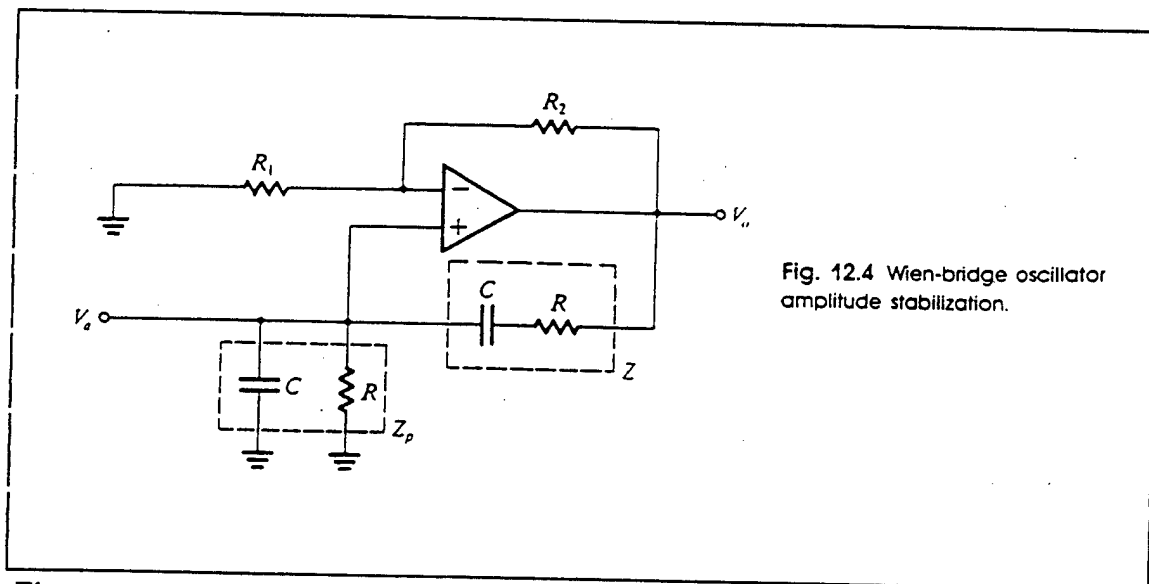


Fig. 12.4 Wien-bridge oscillator amplitude stabilization.

Figure 1.2 From Ref. [5, p.848] Wien-bridge oscillator

Sedra and Smith go on to warn that op amp-RC circuits of this type are only reliable in the neighborhood of 10 Hz to 100 kHz. The lower frequency limit is a function of the passive components used, but the upper limit is a function of the ability of the op amp's slew rate. Simply stated, slew rate is the amount of time the op amp takes to transition from zero to the prescribed voltage of the output, and if this period is long, high frequencies cannot be realized. The fact that

these circuits are unreliable at higher frequencies became a painful reality, and the project was forced to change direction.

The direction taken relied upon the fact that LC and crystal oscillator circuits provide for a better frequency response. They are able to accommodate frequency ranges up to hundreds of MHz. Sedra and Smith go through a detailed description of a Colpitts oscillator [Ref. 5: p. 855]. The oscillator used for the detection side of the circuit is a variation of this circuit. An op amp was chosen for the metal detector circuit due to the fact that an op amp has better tolerance of heat fluctuations than that of the FET (field-effect transistor) used in Sedra Smith example.

Crystal oscillators are generally constructed of a piezoelectric crystal, like quartz, that has electromechanical-resonance characteristics when voltage is applied. The advantages of this device is that it is extremely stable with time and in the face of temperature variations. Also, crystal oscillators have a very high Q factor, which means they are very stable in frequency. The disadvantage of this oscillator is that it is set at a particular frequency and cannot be changed.

### **3. Filters**

In the mine detection circuit to be discussed later, filtering is necessary because the output is meant for a robot and not a human operator like the circuit discussed in the twin oscillator section above. Because of this, the robot does not have ears to filter out the unwanted "sum of frequencies" component.

Signals are sometimes composed of several different frequencies. In order to neglect the unwanted frequency components, first order filters are used. The part of the spectrum that is allowed through the filter is the passband, and the range of frequencies stopped by the filter is called the stop-band. In figure 1.3, a lowpass filter and a highpass filter are drawn to demonstrate the principle.

[Ref. 5, p. 764].

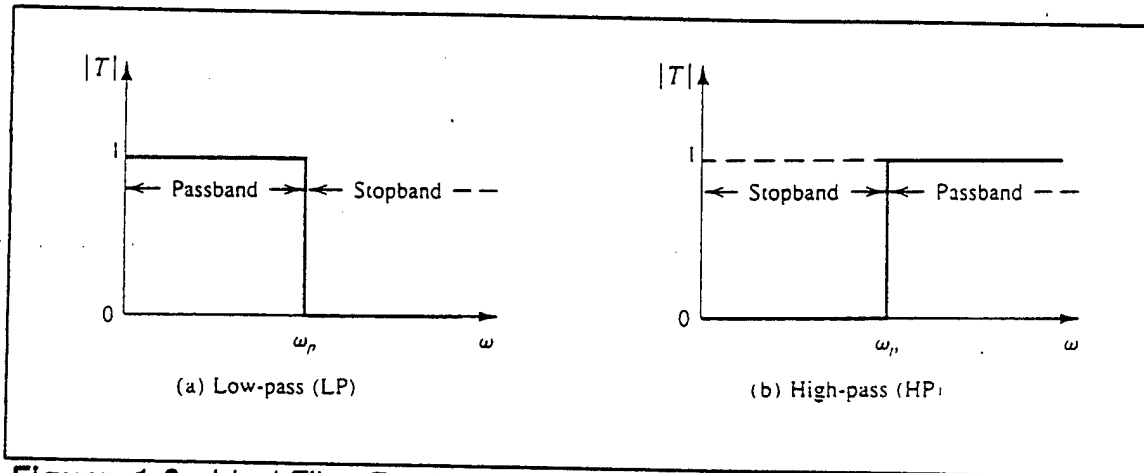


**Figure 1.3** Ideal Filter Realizations

The  $\omega_p$  represents the passband edge. This figure is an ideal representation of a lowpass and highpass filters. In the physical world it is impossible to realize a filter with a vertical passband / stopband division. The order of the filter determines the slope of that line. The higher the order, the steeper the division line. For the purposes of this discussion, first order filters are used, because the attenuation rolloff is not critical. Figure 1.4 displays a table showing different ways to realize a first order filter. The passive filter has been chosen because passive filters are not as restricted by bandwidth.

Filter Type and $T(s)$	s-Plane Singularities	Bode Plot for $ T $	Passive Realization	Op Amp-RC Realization
(a) Low-Pass (LP) $T(s) = \frac{a_0}{s + \omega_0}$			<p><math>CR = \frac{1}{\omega_0}</math> dc gain = 1</p>	<p><math>CR_2 = \frac{1}{\omega_0}</math> dc gain = <math>-\frac{R_2}{R_1}</math></p>
(b) High-Pass (HP) $T(s) = \frac{a_1 s}{s + \omega_0}$			<p><math>CR = \frac{1}{\omega_0}</math> High-frequency gain = 1</p>	<p><math>CR_1 = \frac{1}{\omega_0}</math> High-frequency gain = <math>-\frac{R_2}{R_1}</math></p>
(c) General $T(s) = \frac{a_1 s + a_0}{s + \omega_0}$			<p><math>(C_1 + C_2)(R_1 // R_2) = \frac{1}{\omega_0}</math>  <math>C_1 R_1 = \frac{a_0}{a_1}</math>            dc gain = <math>\frac{R_2}{R_1 + R_2}</math>            HF gain = <math>\frac{C_1}{C_1 + C_2}</math></p>	<p><math>C_2 R_2 = \frac{1}{\omega_0}</math>  <math>C_1 R_1 = \frac{a_0}{a_1}</math>            dc gain = <math>-\frac{R_2}{R_1}</math>            HF gain = <math>-\frac{C_1}{C_2}</math></p>

Figure 1.4 First Order Filter Realizations from Ref. [5, p. 779]

#### 4. Digital Logic

The finished circuit turns the analog input signal into a digital output . Two types of digital logic devices are used. Exclusive-or gates and D Flip-Flops are the means by which the analog signal is converted into digital. The discussion that follows is by no means all inclusive of the functionality of these two logic devices, but does provide the basis for understanding later discussion of their implementation in the circuit.

D Flip-Flops are digital logic devices that can be used to divide a frequency by two. The D Flip-Flops utilized in this thesis are edge-triggered devices. This means that the logic is activated by the rising edge of an input signal. There are two inputs to the D Flip-Flop (the clock and the D). There are also two outputs to a D Flip-Flop (Q and Q'). Figure 1.5 shows the truth table for the D Flip Flop. By placing the periodic signal of the frequency to be divided onto the clock input of a D Flip-Flop, the low to high transition supplies the edge-triggering mechanism for the rest of the Flip-Flop. By using the incoming signal as the trigger and attaching the D input of the Flip-Flop to the Q' output (Q' being the inverse of the output Q), the incoming frequency is effectively divided by two. This occurs because, as Figure 1.5 shows, the output , Q, assumes the value waiting at the D input each time the clock is triggered. The new Q' value is then fed back to the D input. It is important to note that as the clock transitions from high to low, the

Q is unchanged, and is in the memory state. An example of the divide by two follows:

$D=R=S=Q'=0$  and a low to high transition occurs. Now,  $Q=0$ , and  $Q'=D=1$ .

The clock transitions high to low with no change in output, it is still high. The next low to high transition occurs,  $Q=D=1$ ,  $S=R=Q'=0$  and the output is now low.

Note that two input low to high transitions produce only one low to high output.

The first low to high transition of the clock makes the output  $Q'$  high, and the next low to high transition forces  $Q'$  low.

Figure 1.6 shows the divide by two D-Flip-Flop circuit implemented.

clock	D	S	R	Q	Q'
↑	0	0	0	0	1
↑	1	0	0	1	0
↓	X	0	0	Q	Q'

Figure 1.5 D Flip Flop Truth Table

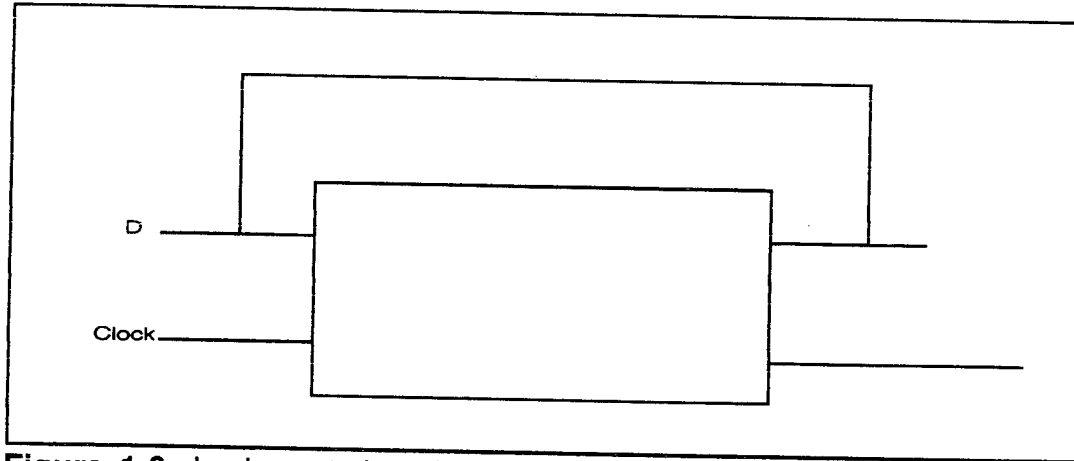


**Figure 1.6** Implementation of a D Flip-Flop in a Divide By Two Circuit

The exclusive-or function is a unique logic function that follows the following rules:

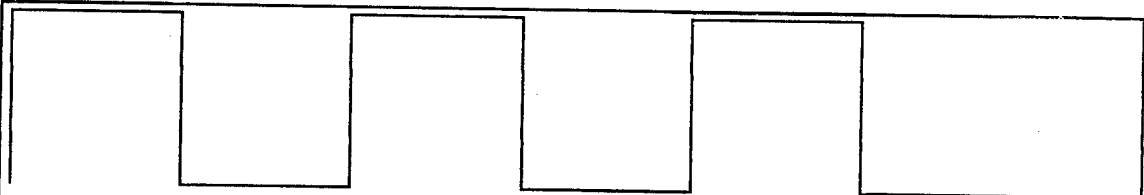
- 1) if the inputs are the same, the exclusive-or output is a logical zero;
- 2) if the inputs are different, the exclusive-or output is a logical one.

This truth table makes the exclusive-or gate useful for a variety of functions.

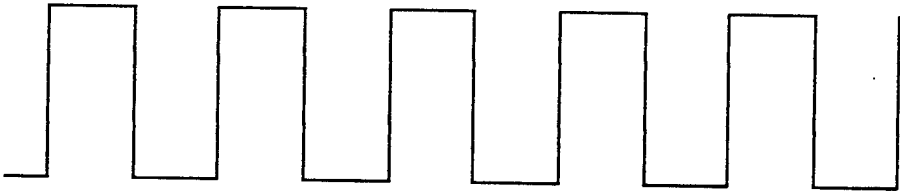
Of primary interest is the use of the exclusive-or gate to combine two fifty percent duty cycle signals. In this capacity, the exclusive-or function behaves as a mixer in communications theory. It provides a nonlinear combination of signals, and performs the time domain function of multiplication. When periodic signals of different frequency are multiplied in the time domain, the result in the frequency domain is a signal that possesses two distinct parts. The output frequency possesses a component that is the sum of the two signals, and a component that is the difference of the two signals. Figure 1.7 shows a demonstration of this fact.

In this diagram a one Hz signal (a), is combined with a two Hz signal (b) using the exclusive-or function. The output is demonstrated in (c). If the theory that it behaves as a mixer is correct, the output should be a 3 Hz signal component (the sum of the two frequencies), and a one Hz frequency (the difference of the two frequencies). Part (c) of the diagram shows that in a one second interval, these component parts do exist. The shaded areas represent the sum of frequencies, and the white areas represent the difference frequency. As explained earlier, it does behave as a mixer.

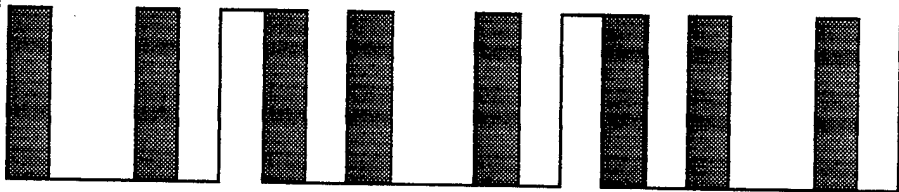
The first chapter of this thesis discusses the principles required to understand the construction of the sensor. The second chapter addresses the construction and design considerations that went into the circuitry of the sensor. The third chapter discusses the testing procedure and results. The fourth chapter draws out some of the applications of this sensor and mentions work that is currently in progress to use the results of this thesis.



a) One Hz signal



b) Two Hz signal



c) Exclusive-or output

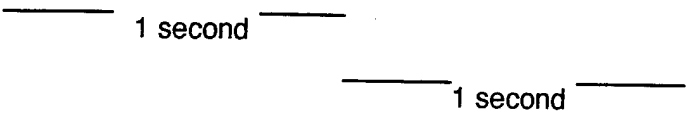


Figure 1.7 Exclusive-or Function Used as a Mixer

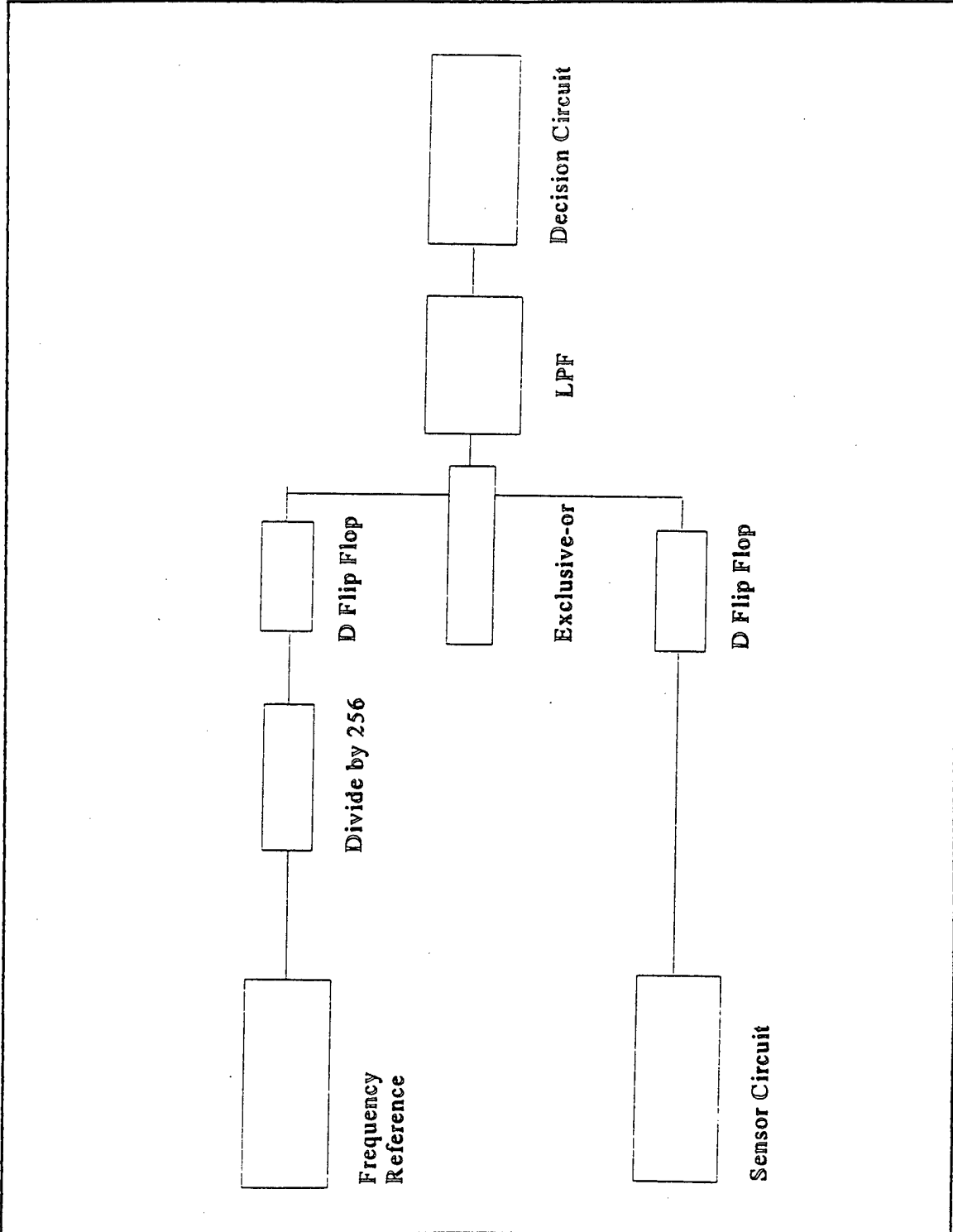


## II. DESCRIPTION OF THE SENSOR

### A. PRINCIPLE

The sensor which is analyzed in this thesis is a twin-oscillator design. Figure 2.1 gives an overall block diagram of the circuit. As such, the circuit is divided into two distinct sections. One side will be named the frequency reference side, and the other side will be referred to as the sensor side. This circuit generates a reference frequency through the use of a crystal instead of the tunable inductor / capacitor combination that is discussed in the Literature Review Section above. Unlike the circuit of Reference 3 where the coils are tuned in frequency to be 1 kHz apart, the reference frequency in this circuit is matched exactly by the sensor side through the use of a tunable inductance coil in combination with correct capacitance. The frequency reference side of the circuit is then combined with the sensor side of the circuit through an exclusive-or function. While these two frequencies are the same, the exclusive-or output will contain a DC component and an AC component. If on the other hand, the coil on the sensor side of the circuit passes over metal, the inductance that the circuit sees goes up, and according to the equation  $\omega^2 = 1 / LC$ , the frequency goes down, thus creating a difference frequency out of the exclusive-or gate. The exclusive-or gate performs the role of a mixer. As demonstrated earlier, it creates the same effect in the frequency domain as multiplication in the time domain, in that the frequencies coming into the exclusive-or gate produce an

Figure 2.1 Overall Circuit Block Diagram



output of the sum and the difference of the individual frequencies. The higher frequency, i.e. the sum of the two frequencies is filtered out using a simple first order filter, thus leaving only the difference frequency. This difference frequency is then sent to the rest of the circuit for processing. The two outputs of this circuit are a flashing light, and a binary voltage output for later input to an autonomous robot.

## **B. IMPLEMENTATION**

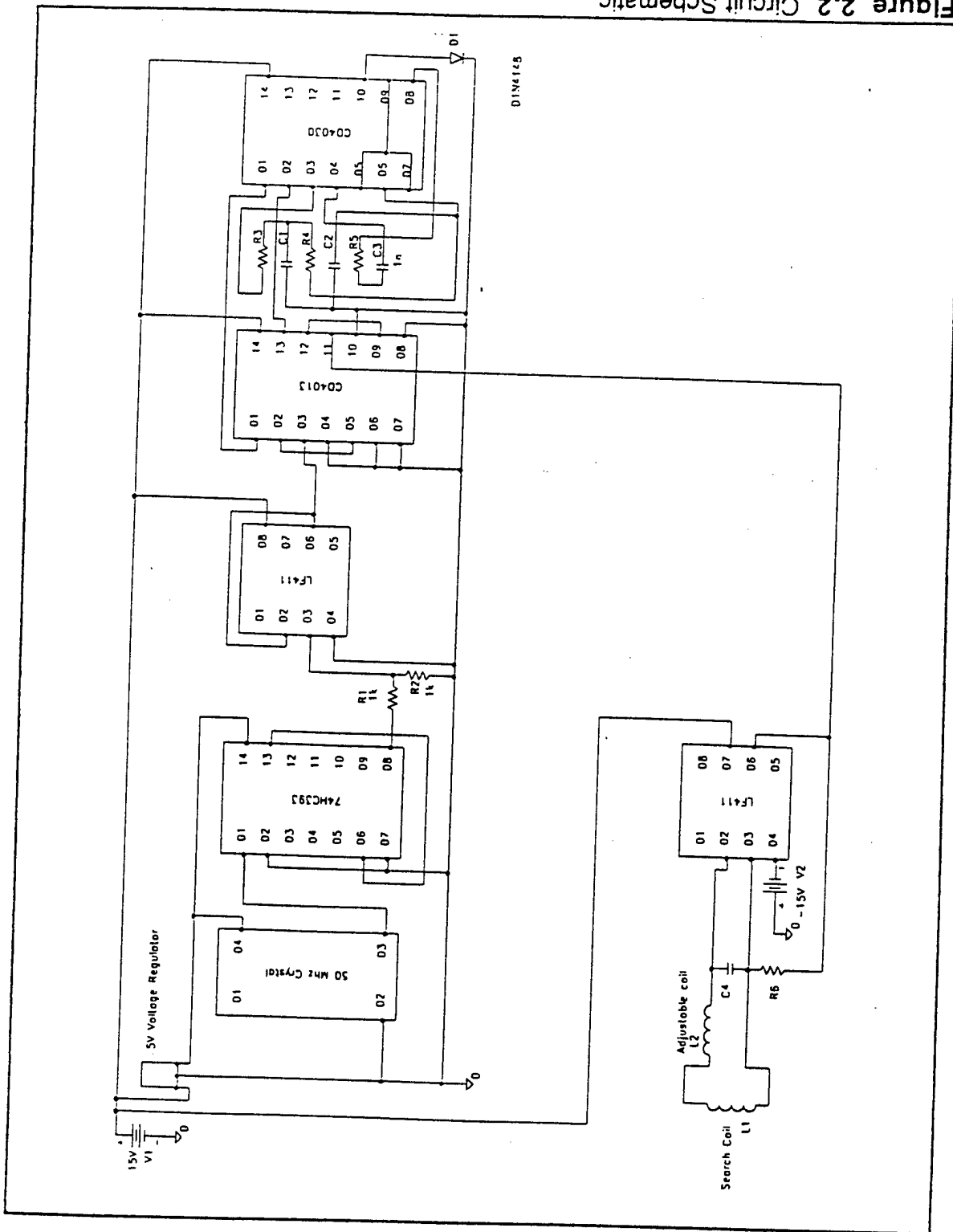
This section will address the implementation of this metal detection circuit described above. In this section, the parts and design considerations will be discussed in great detail to ensure that the reader understands the process and the issues of design. A detailed drawing of the circuit is supplied in Figure 2.2. The actual values to be used will be presented in the next chapter discussing the results of testing.

### **1. Power**

Power begins with a 15 Volt bus that is distributed to all of the C-MOS 4000 series chips (CD4013, CD4030), and the two LF411 op-amps. The 15 Volt bus also delivers power to the (LM317T) 5 Volt voltage regulator.

This 5 Volt regulator runs the non C-MOS system components (the 50 MHz crystal oscillator and the 74HC393). It is necessary to attach a capacitor to the output of the 5 Volt regulator because its output was noisy, and disrupted the logic gates that followed.

Figure 2.2 Circuit Schematic

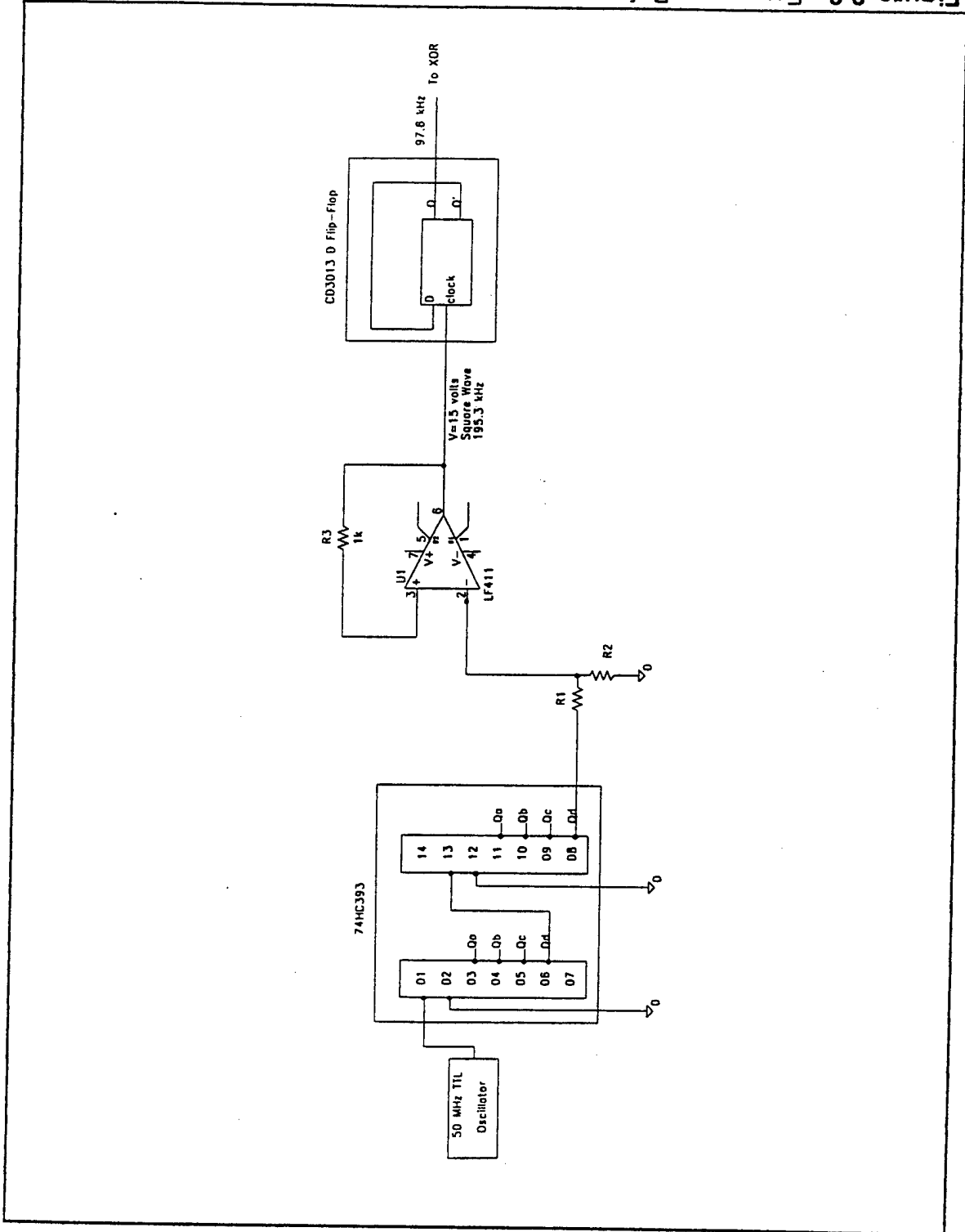


A negative 15 Volt bus is also required to insure correct function of the sensor side of the circuit. The LF411 was originally connected with a positive 15 Volts into pin 7 with pin 4 tied to ground. The resulting problem was that the output signal was not symmetric enough to obtain a correct output from the dual D Flip-Flop (CD4013B). By forcing the low voltage to negative 15 Volts, the problem was solved. The positive voltage must be nearly symmetric to the negative voltage for correct operation.

## **2. Frequency Reference Side**

The frequency reference side is crucial to the sensitivity of this metal detecting device. Figure 2.3 shows a detailed design of the frequency reference side of the circuit. After many attempts at creating an oscillator that remains stable even at high frequencies, a crystal oscillator was chosen. Many attempts were made at using RC configurations in Reference 5, but none of them proved to be as stable as what is constructed here. This is an important factor, because when adjusting two oscillator frequencies to be exactly the same, the less the drift, the better the result. As will be explained later, having two oscillators that have drift, no matter how small, negates the sensitivity of the circuit, and does not allow for premium performance. The sensor side of the circuit must contain an inductor, therefore it is susceptible to drift. For this reason it is of the utmost importance that the frequency regulator side of the circuit does not drift.

Figure 2.3 Frequency Reference



As explained earlier, a crystal has a very precise, mechanical production of a voltage pulse. This pulse is extremely accurate, but cannot easily be altered. The idea is to use this mechanical pulse as the clock input into the 74HC393, which will divide the original crystal parameter by 256, thus giving flexibility to the crystal oscillator. This divider is capable of handling this frequency, and provides little to no frequency drift.

After the dividing down circuit is completed, the output goes to an LF411 which amplifies the signal, it then serves as the clock to a Dual D Flip-Flop (CD4013B). The function of the Dual D Flip-Flop is two fold. First, it divides the incoming signal by two, and second it preconditions the signal by creating a fifty percent duty cycle for the outgoing signal. Fifty percent duty cycle means that it is logically high for the same amount of time it is low.

The output of the D Flip-Flop goes into one gate of the exclusive-or chip. It is at this point that the reference frequency is compared with the sensor frequency via the exclusive-or function.

The values for the resistors in this drawing are,  $R1=R1=5.1k\Omega$ , and  $R3=50\Omega$ .

### **3. Sensor Side**

The sensor side uses an op-amp version of a Culpitts oscillator. Figure 2.4 shows the arrangement of the parts. The coil is attached to the circuit via 6 feet of coaxial cable to reduce any outside inductance that may be acquired by the connection.

The equation for the frequency of oscillation remains the same:

$$\omega^2 = 1 / LC$$

where  $\omega = 2\pi f$ .

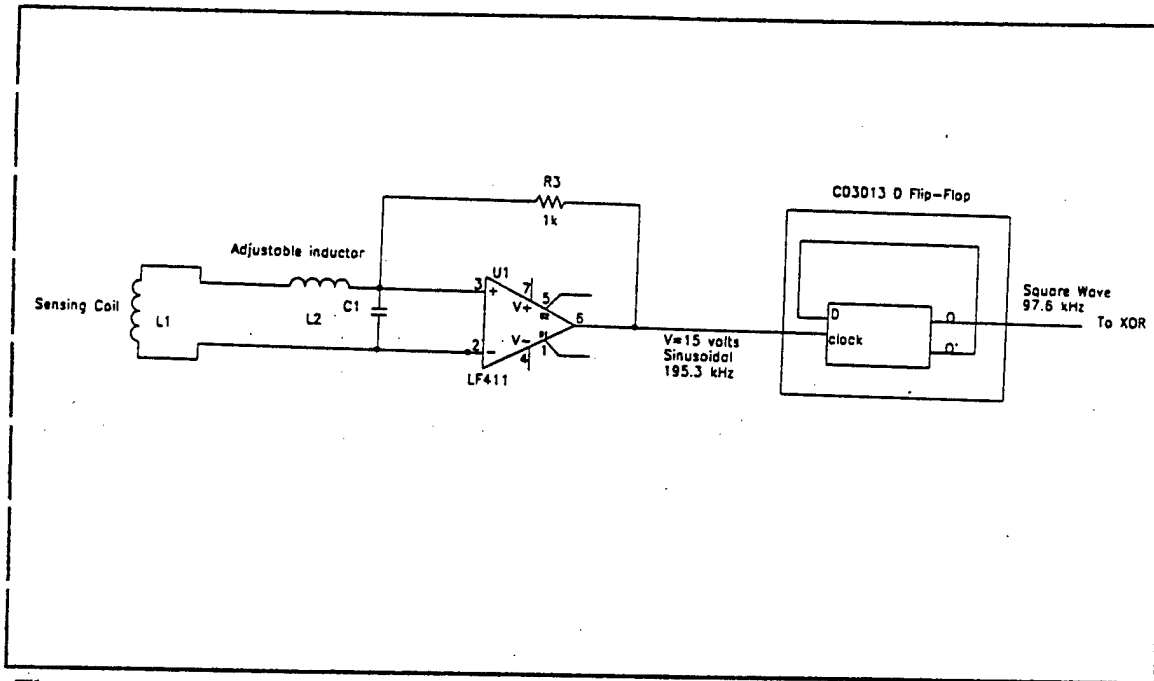


**Figure 2.4** Sensor Circuitry

The inductance is supplied through a coil of 30 gauge wire, and the capacitance is manipulated through a parallel series of capacitors. One of the purposes of the thesis is to evaluate performance of the circuit, having different inductor coil sizes and coils with different numbers of turns, so this 30 gauge coil will be wound with several different numbers of wraps.

The resistor in the figure is theoretically not required, but in practice, a feedback resistor must be placed between the output and the positive terminal of the input in order to provide a trickle of current required to sustain oscillation.

Another feature of the circuit is the appearance of an adjustable  $36 \mu\text{H}$  inductor in series with the coil. This coil is to be utilized as a tuning coil. Sometimes it is impossible to obtain the exact capacitance / inductance combination to provide the exact frequency of the reference frequency side. This tuning coil allows the exact frequency to be attained by adding inductance to the circuit after it has been tuned as closely as possible to the reference frequency side without the tuning coil. As a general guideline, it can tune the circuit about 150 Hz.

The output of the LF411 op-amp provides the clock for a D Flip-Flop. A sine wave is exiting the op amp. If this wave were to be sent directly to the exclusive-or gate to be compared with the reference side of the circuit (a square wave), depending upon the phase the output of the exclusive-or gate could give a false detection. While a sine wave appears almost square, the difference in shape may produce an error. Again, this Flip-Flop preconditions the signal in voltage, but more importantly gives it a fifty percent duty cycle square wave output. The Flip-Flop output provides the other input to the exclusive-or gate, where it is combined with the preconditioned frequency reference side of the circuit. The realization of this circuit is very dynamic. As the frequency of the circuit is adjusted and the number of turns (N) are changed for testing purposes, the amount of capacitance represented by C1 and the feedback resistor in Figure 2.4 must be adjusted accordingly. As frequency increases, C1 decreases. As the number of turns increases, the inductance increases, and C1 decreases.

Figure 2.5 shows the values of the feedback resistors as tested in the circuit.

	25 turns	50 turns	75 turns	100 turns
195 kHz	5 k $\Omega$	10 k $\Omega$	-	-
97 kHz	2 k $\Omega$	4 k $\Omega$	5 k $\Omega$	-
48 kHz	-	3 k $\Omega$	3 k $\Omega$	300 $\Omega$

**Figure 2.5** Values of the Feedback Resistor for each Circuit Combination

Figure 2.6 shows the actual capacitor values (C1) used in testing the circuit. If the resistor value and corresponding capacitance values are placed in the circuit, the circuit will be close enough to matching the reference side frequency to the sensor side frequency that the tunable inductor on the sensor side may be used to exactly tune the circuit. Tuning of the circuit will be explained in more detail in Section 6 of this chapter.

Frequency=195.3 kHz

Diameter	N=25	N=50	N=75	N=100
12	.10e-8	-	-	-
10	.115e-8	-	-	-
8	.169e-8	.059e-8	-	-
6	.330e-8	.056e-8	-	-
4	.364e-8	.094e-8	.05e-8	-

Measured capacitance in Farads

Frequency=97.6 kHz

Diameter	N=25	N=50	N=75	N=100
12	-	-	-	-
10	.050e-7	.135e-7	-	-
8	.066e-7	.018e-7	-	-
6	.076e-7	.027e-7	.013e-7	-
4	.125e-7	.029e-7	.033e-7	-

Measured Capacitance in Farads

Frequency

Diameter	N=25	N=50	N=75	N=100
12	-	.050e-7	.026e-7	-
10	-	.061e-7	.028e-7	-
8	-	.077e-7	.378e-9	-
6	-	.109e-7	.986e-9	13e-9
4	-	.180e-7	11e-9	14e-9

Measured Capacitance in Farads

Figure 2.6 Actual Capacitances as Tested in the Circuit

#### 4. Output Signal Circuitry

Figure 2.7 shows the signal decision section of the circuit. As explained earlier, the exclusive-or function behaves much as a mixer in communications. When the sensor signal and the reference signal are not exactly the same, the exclusive-or gate will produce a sum and a difference frequency. Since a light emitting diode is used to show detection, and a spectrum analyzer with a maximum frequency of 20,000 Hz was available, the decision to filter the high frequencies was made. To accomplish the filtering, two simple first order, low pass, passive filters of resistor / capacitor construction were cascaded to attenuate the unwanted high frequencies. The cutoff frequency for these filters is approximately 24 kHz ( $\omega=1/RC$ ). A single stage filter was not enough to prevent the exclusive-or gate which follows from amplifying the high frequency component. After the filters, the signal is then sent into an exclusive-or gate in which one of the leads to the gate is tied low. From the exclusive-or truth table it is obvious that any input sent through an executive-or gate with zero as the other input, provides an output exactly like the input. The point to using the exclusive-or gate in this position is that it will behave as an amplifier without changing the incoming signal. The signal leaves this exclusive-or gate and enters a first order high pass filter. The purpose of this filter is to eliminate any DC component that may have entered the system. As discussed earlier in the thesis, a DC component is produced when two square waves are sent through an exclusive-or gate.

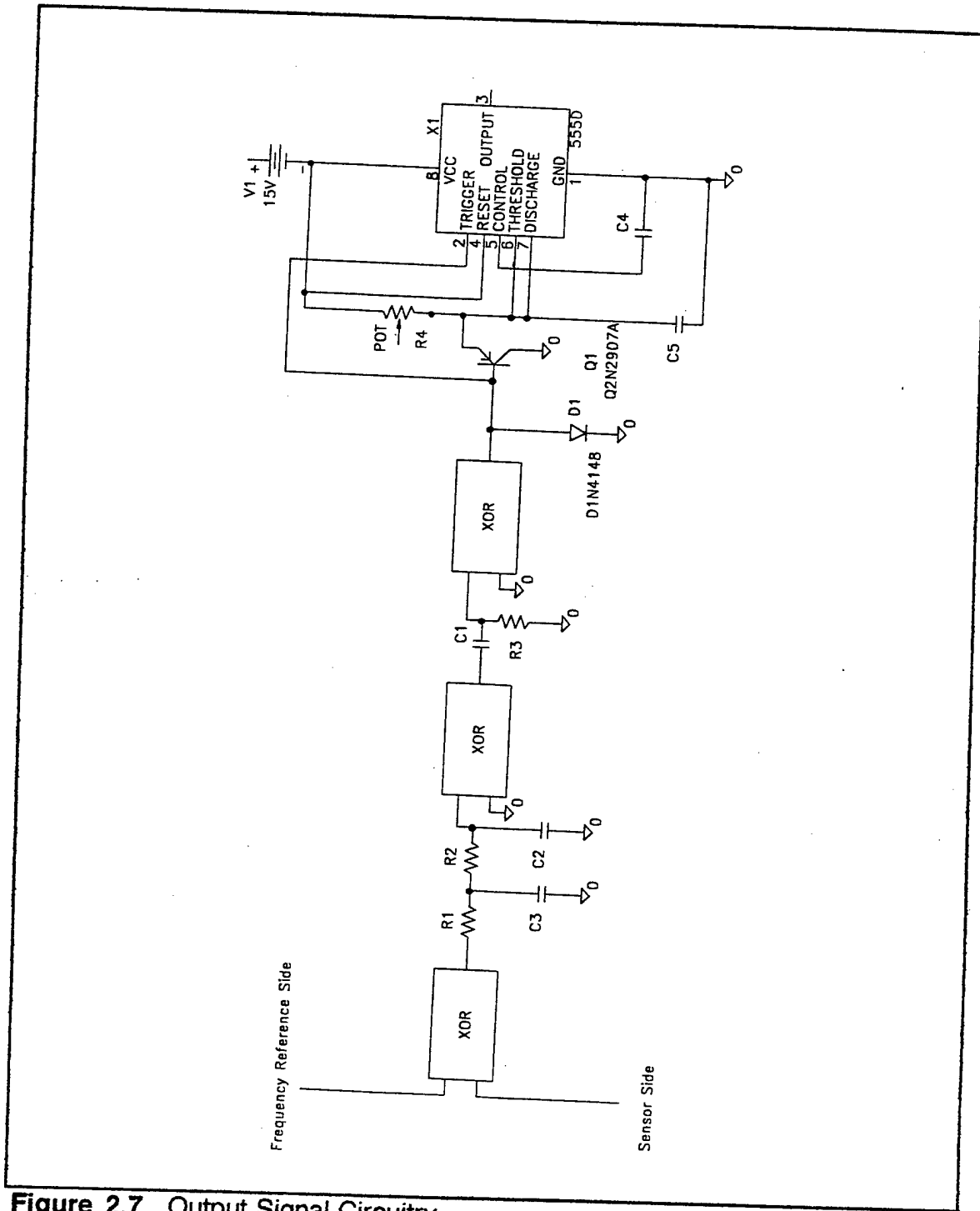


Figure 2.7 Output Signal Circuitry

If they are in phase they will produce a DC voltage of zero out of the exclusive-or gate. If, however they are exactly 180 degrees out of phase, the high voltages will add, and produce a strong DC voltage. Since the phase of the square waves is unpredictable and the circuitry required to align them is difficult to build, a high pass filter is placed here with the cutoff frequency as close to zero as possible. The signal then enters the final exclusive-or gate in which one of the inputs is tied low just like above, this stage acts as an amplifier for the LED. An LED is placed at the output to show detection. It will flash according to the frequency through the last exclusive-or gate. Again, this frequency represents the difference between the Sensor side and the Frequency Reference side of the circuit. It also becomes clear that the high pass filter is necessary because if the DC voltage is allowed to pass, the indicator light will stay lit whether the sensor is in the presence of metal or not. To provide a logical one or zero as an output, a circuit that involves the use of a FET and a 555 Timer is added.

The actual values of the Output Signal Circuitry diagram shown in Figure 2.7 are  $R1=R2=12k\Omega$ ,  $R3=1M\Omega$ ,  $R4=10k\Omega$ ,  $C1=.2H$ ,  $C2=C3=3500pF$ ,  $C4=C5=.01\mu F$ .

## **5. Frequency Division**

The frequency of the circuit as shown here is considered to be running at 195.5 kHz. The reason for this is that on the Frequency reference side of the circuit, the 50 MHz Crystal oscillator is being divided by 256 using the 74HC393 chip. Although the 195 kHz signal is again divided by 2 before entering the

exclusive-or gate with the Sensor side of the circuit, the point is that in order for the sensor side to match the Frequency reference side, the coil and capacitor must be tuned to 195 kHz because the sensor side also undergoes a final divide by two.

One of the testing criteria for this thesis involves changing the frequency of the circuit to observe the changes in detection range. This is accomplished by adding an N4024 divide by seven counter. This device is placed between the output of the 74HC393 and the LF411 on the Frequency reference side of the circuit. This arrangement is shown in Figure 2.8. This set-up allows for a divide by 2 and 4 capability. Now the circuit can be tested at 97.6 kHz and 48.3 kHz frequency reference respectively.

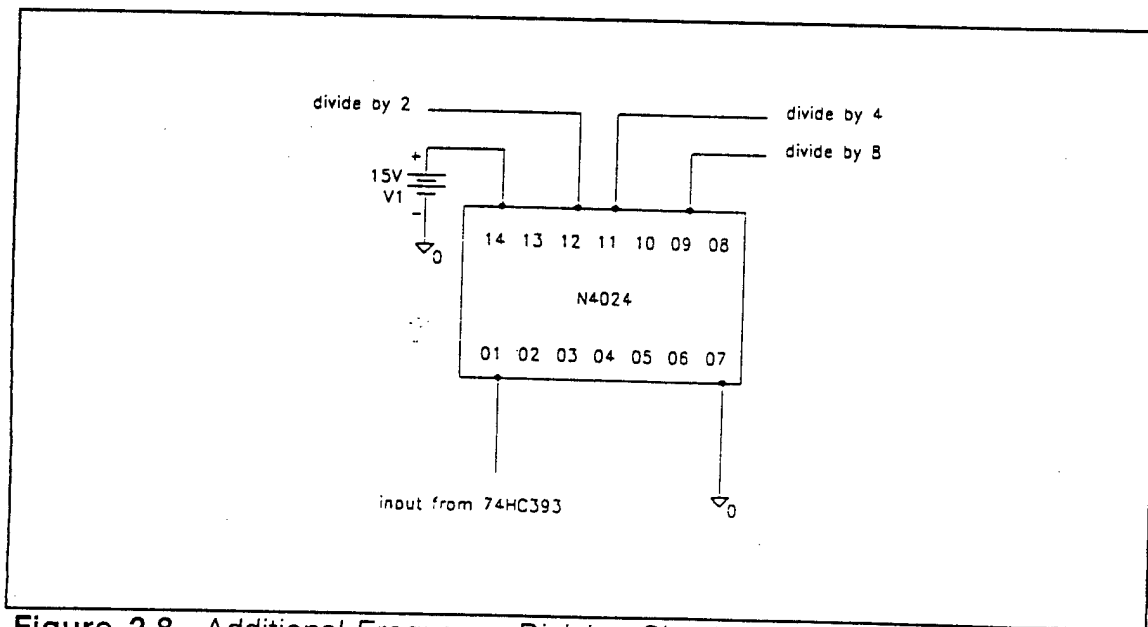


Figure 2.8 Additional Frequency Division Circuitry

## **6. Tuning**

Tuning is accomplished by use of the LED. This procedure is critical in the detection range of the circuit. As it is arranged, the circuit will react if it is influenced by either magnetic or anti-magnetic materials. The output is a shift in frequency seen at the output of the circuit. While the circuit is not influenced by any outside inductance, the LED will remain extinguished as long as the sensor side and the frequency side are operating at exactly the same frequency. To tune this circuit to be sensitive, the tunable inductor must be turned so that the light is flashing very slowly, then turn the adjustment slowly until the LED extinguishes. This assures the user that the circuit is at maximum sensitivity.

This tuner provides another very useful function. It allows the circuit a certain amount of adaptability. While attached to one autonomous robot, the electromagnetic field is set, and the coil can be adjusted accordingly. However, if the sensor is moved to an entirely different environment, or even another autonomous robot, the circuit is not set in stone, and it can be adjusted.

## **7. Shielding**

Previously stated in the assumptions section of the thesis was the fact that the coil is not shielded from electromagnetic fields. This is intentional. The very nature of the coil is that it detects electromagnetic fields. Shielding would hinder performance. Since the exact robot for the mounting of this detector is not yet known, the coil shielding will need to come from the system designer if

the tuning circuit provided is not capable of allowing for the interference that may come from the robot.

The circuitry, on the other hand, should be isolated from external fields. To accomplish this, the circuit was placed inside a metal container which behaves as a Faraday Shield. The connection between the circuit and the coil is constructed of coaxial cable and is relatively resistant to external magnetic fields. A twin axial cable was first used in the circuit and proved to be inadequate. The twin axial cable performed as an antenna and produced many false positive results.



### III. TESTING / RESULTS

#### A. TESTING

A photograph of the circuit is included in Figure 3.1. The circuit is normally encased in a metal container and provided rubber shock mounting that can be screwed on to the bottom of the metal case. The target is a World War II vintage pressure activated mine that is still likely to be found in the field today. This mine can be expected to be located between six inches and one inch under the soil. When a target passes over the mine, the plunger is depressed, activating the mine.

The testing consisted of laying the circular search coil flat, i.e. parallel to the ground, and turning the adjustable inductance coil until the tuning light had extinguished. The target mine was then placed under the coil as close as possible to center. If the coil detected the mine, the target depth was increased. This continued until the circuit no longer detected the mine. Once this distance was determined, the target was physically removed from the environment of the coil to see if the detector returned a non detection. If so, the target was replaced at the same distance to verify detection. If the circuit again returned a detection signal, this depth was recorded.



**Figure 3.1** Photograph of Circuit

## **B. RESULTS**

### **1. Data Obtained**

The results of this study quantitatively come down to depth, and the effect that different elements have on the depth. I have gathered data on the number of turns, the diameter, and the frequency of operation of oscillators and have compiled Figure 3.2 to display the results. This tables in this figure represent repeatable results obtained by the process described above. Sometimes the tuning of the circuit may be more sensitive than normal, and this allows for the ranges attained by the circuit to be greater than the distance reported here, but the distance reported here represents the distance which the circuit could be built, measured, and rebuilt and still obtain this range of detection. Figures 3.3 through 3.5 demonstrate the most telling results. These six plots show the relationship between the diameter of the coil, and the depth at which it can detect the target.

The other factors such as number of turns and frequency of operation do not provide interesting plots. The trend seems to be that the number of coils somewhat increases the detection depth, but the frequency of oscillation has little to do with detection range.

As is evident from the eight diameter vs. depth graphs, the depth seems to follow a somewhat linear relationship with the diameter of the coil. As the coil diameter increases, the depth also increases.

Frequency=195.3 kHz

Diameter	N=25	N=50	N=75	N=100
12	14	-	-	-
10	13	-	-	-
8	9.75	10.5	-	-
6	8	7	-	-
4	5.5	6	5.5	-

Frequency=97.6 kHz

Diameter	N=25	N=50	N=75	N=100
12	13	-	-	-
10	12	12	-	-
8	9.75	10.25	-	-
6	7.5	8.25	8	-
4	4.5	7	7	-

Frequency=48.8 kHz

Diameter	N=25	N=50	N=75	N=100
12	-	14.75	16.25	-
10	-	14.25	12.75	-
8	-	11	11	-
6	-	7	9	8
4	-	6.5	6.25	7

Figure 3.2 Tabulated Results

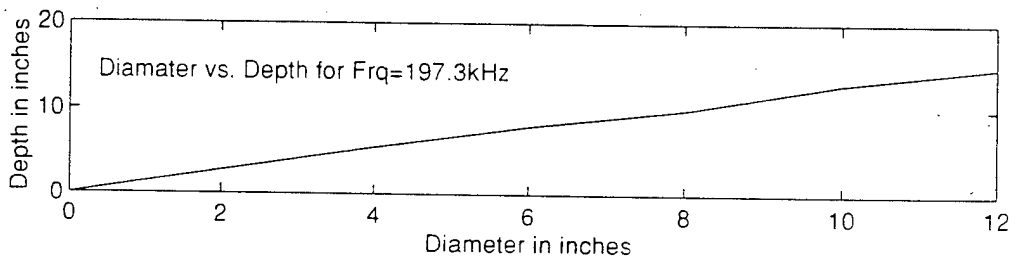
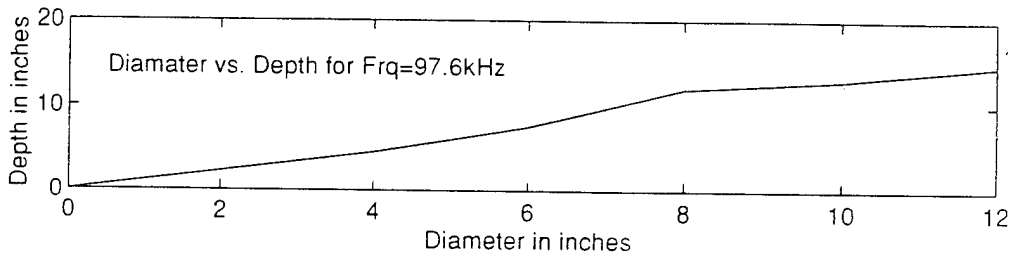
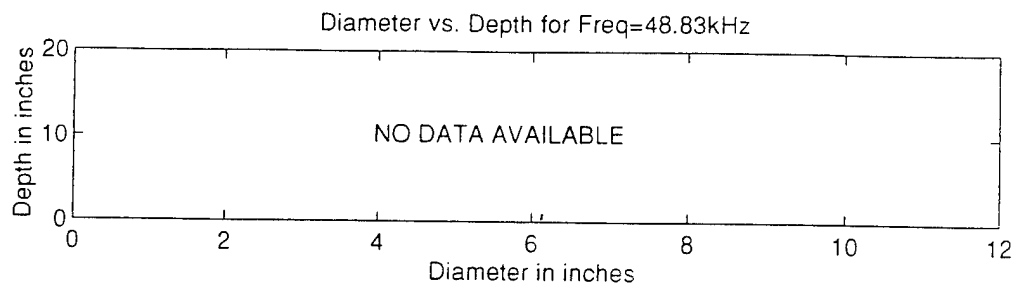
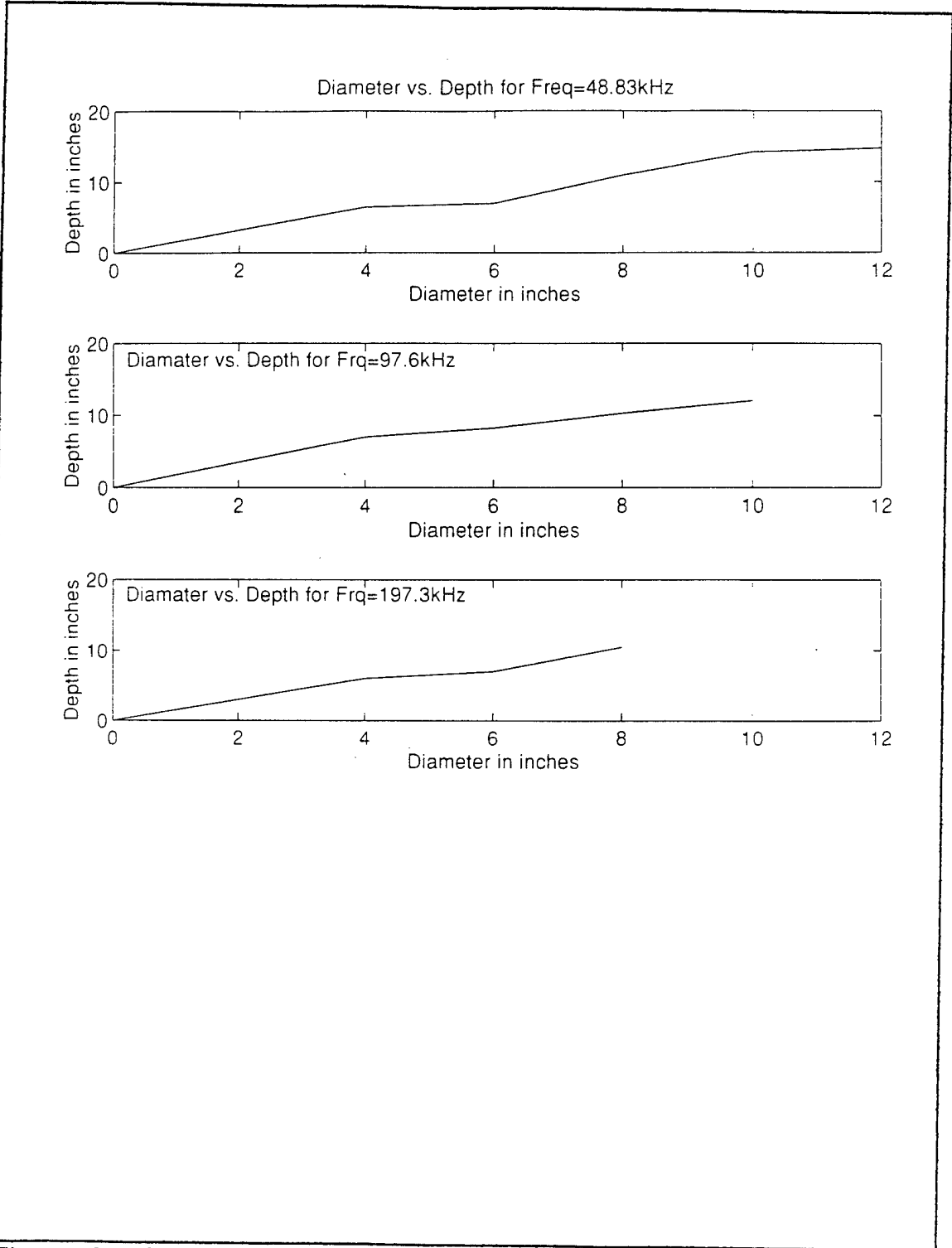


Figure 3.3 Graph of Diameter vs. Depth for N=25 Turns



**Figure 3.4** Graph of Diameter vs. Depth for N=50 Turns

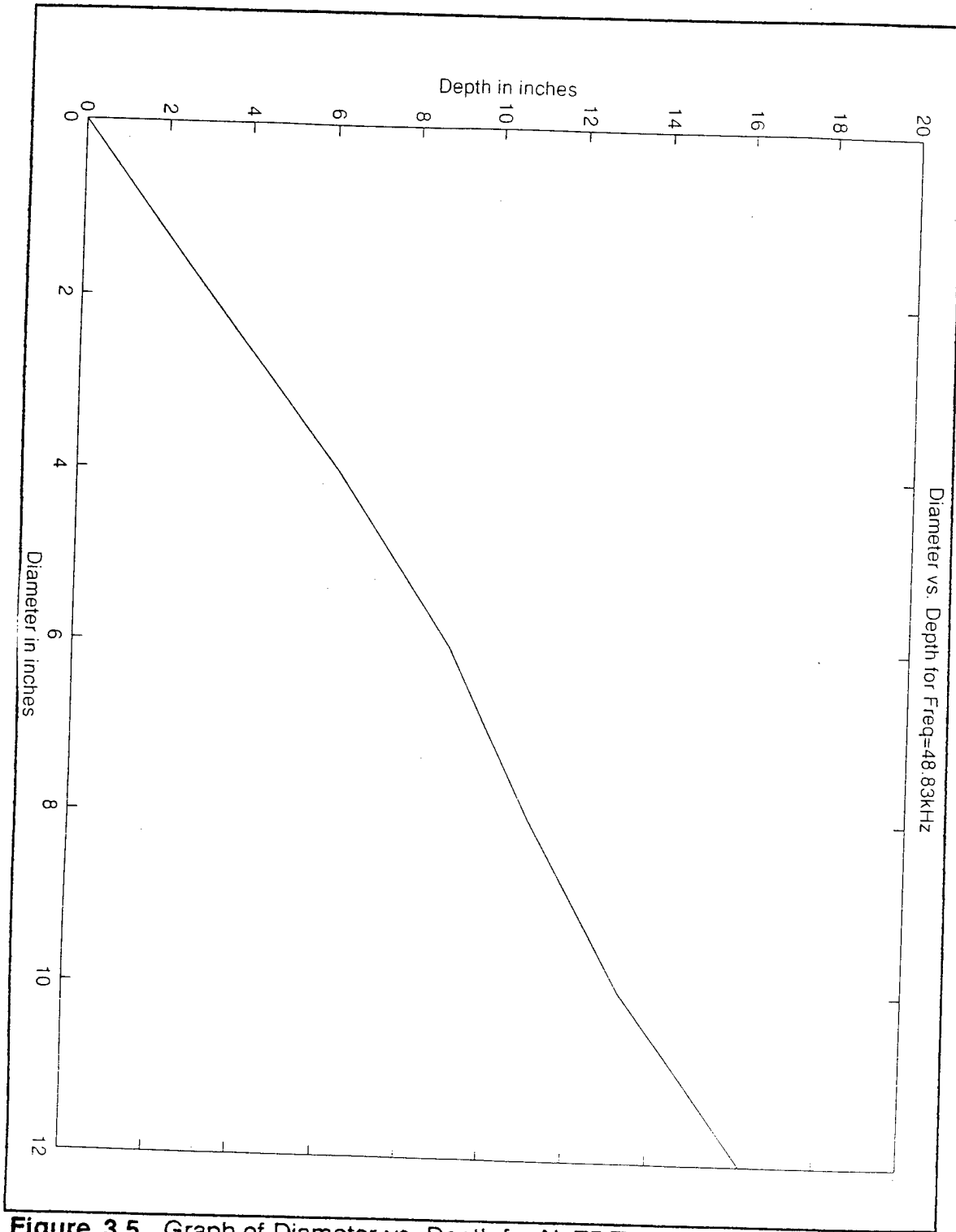
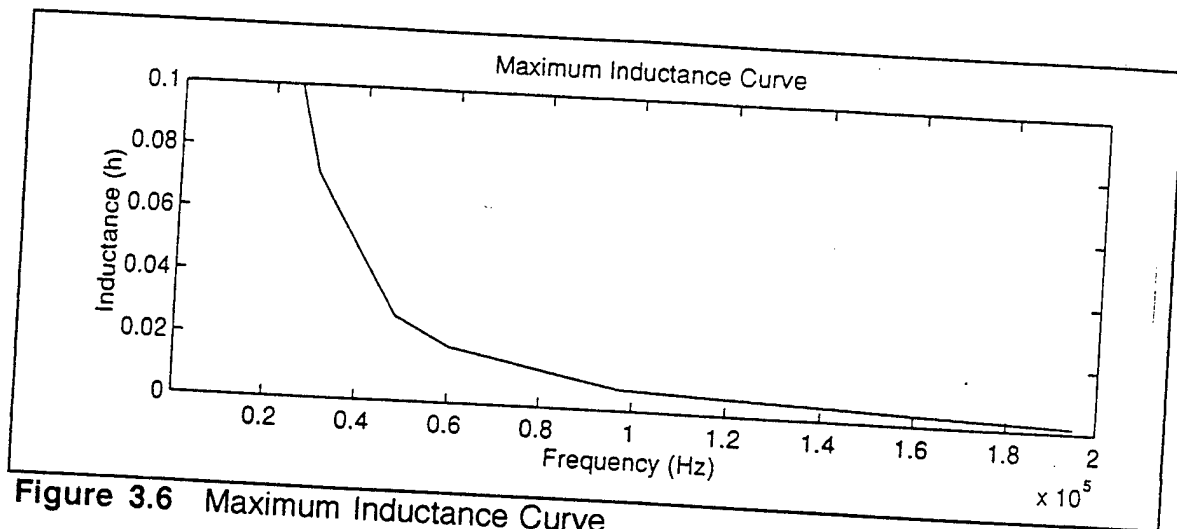


Figure 3.5 Graph of Diameter vs. Depth for N=75 Turns

## 2. Data Discrepancies

It is important to note that the board itself has a capacitance of 25 pF, and the board with 6 feet of coaxial cable has a capacitance of 690 pF. This is an important fact because it is directly related to the collection of data. Knowing that  $\omega^2 = 1/LC$ , if the capacitance (C) is a minimum value, there exists a limit upon the maximum inductance from the coil itself. Figure 3.6 demonstrates this curve. The result is that the cutoff inductance for 195.3 kHz is .0017 H, for 97.6 kHz is .0068 H, and for 48.8 kHz is .027 H. Accordingly, large coils and coils with many turns may have too much inductance and cannot be used on this circuit board. In the data that follows, you will see that some data was not recorded. This is a direct reflection on the intrinsic capacitance of the circuit limiting the amount of inductance that allows the frequency of the sensor side to be initially greater than or equal to that of the frequency reference side. If this condition is not met, the two frequencies cannot be adjusted to be exactly the same, because the only adjustment available is to add capacitance or inductance to the circuit. Both of these parameters slow the frequency of the sensor side, and if it is too slow to begin with, the frequencies will never be matched.



**Figure 3.6** Maximum Inductance Curve

The data collection at  $N=25$  at 48 kHz is a special problem. The reason this data was not collected is that the circuit could not be made stable. As previously mentioned, the op amp feedback resistor on the sensor side assumes different values for different sizes of coils and for different frequency realizations. In this isolated case, a very small resistor (along the order of  $20\Omega$ ) could get some oscillation but it could not sustain any steady frequency. This resistor value pushes the current to high levels and is not advised in the circuit. The circuit was deemed "unstable," and the data was discounted as unreliable.

Faced with the inherent 390 pF of capacitance on the board, the inductance of each coil was computed using the formula  $L=1/\omega^2C$ . The capacitance used in each circuit was measured. The result of the actual capacitance measurement is tabulated in Chapter II. This was applied to the above formula, and an inductance was arrived upon. A self inductance formula was attained from Reference 8 to be:

$$L = N^2 r^2 / 9r + K$$

where N represents the number of turns, r is the radius of the coil, and K is a constant that depends upon the width of the wire involved in the wrapping. This formula, however, did not fit the empirical findings.

Using the above formula as a starting point, the following formula was used as the basis for a least squares solution for the inductance.

$$L = N^2 r^2 / a_1 N^2 r + a_2 N r^2 + a_3 N r + a_4 N^2 + a_5 r^2 + a_6 N + a_7 r + a_8$$

After running a least squares solution for all of the empirical data, the final coefficients for inductance are in Figure 3.7:

a1	21.9	a5	38.7e6
a2	-2.62e6	a6	-29.5e6
a3	829000	a7	-888e6
a4	-25450	a8	655000

**Figure 3.7** Least Squares Coefficients

These coefficients needed to be normalized by multiplying the equation by a factor of -200. After this coefficient is applied, the Least squares curve is close to the inductance curve resulting from the empirical results. Figure 3.8 demonstrates the difference between the least squares curve and the measured data.

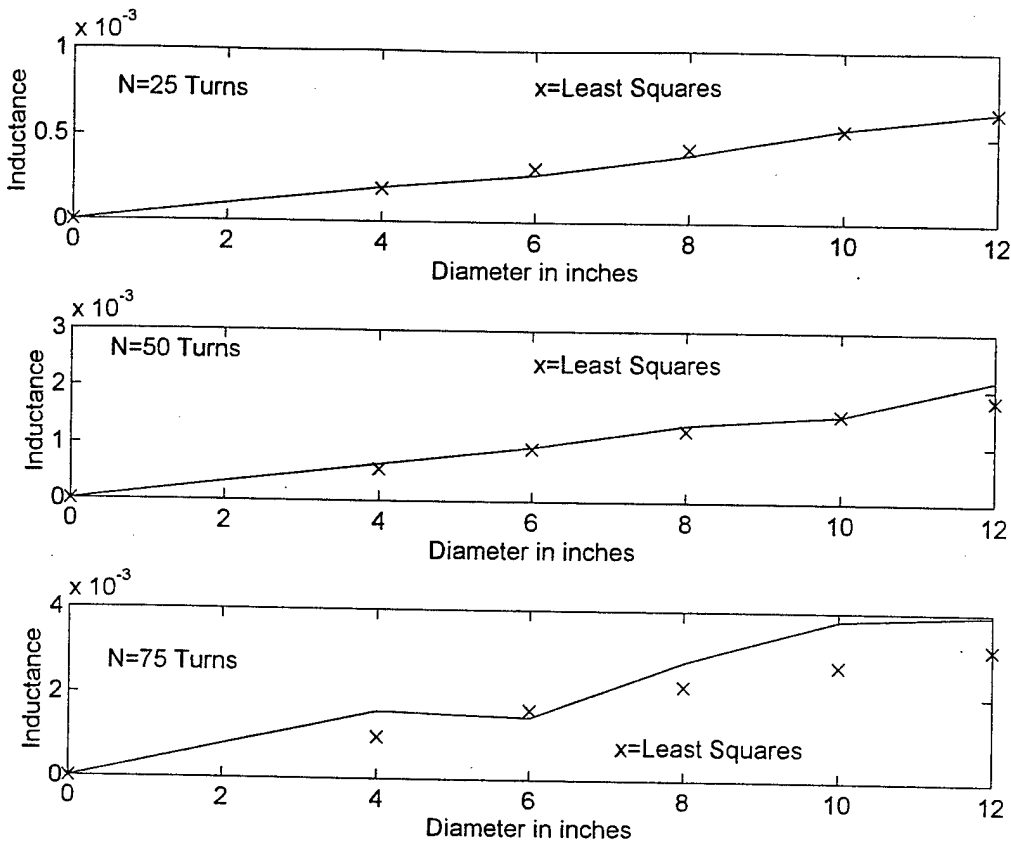


Figure 3.8 Least Squares Formula vs. Empirical Data for Inductance

### **Figure 3.8** Least Squares Formula vs. Empirical Data for Inductance

Figure 3.8 provides curves for inductance look-up. This allows easy solving of the capacitance required for a particular sensor coil size, vice the trial and error approach used in the data collection for this thesis. For the sizes of coils presented in this thesis, the tables in Chapter II will suffice for reconstruction of the circuit. If a different coil is to be used, this formula provides a good starting point.

### **3. Conclusions**

The design is successful. A lightweight device has been engineered to display the desired characteristics. It is low power. Mostly C-MOS chips are utilized to reduce the power consumption of the circuit. The circuit itself can be run on any positive and matching negative power supply between 5 and 15 volts. The circuit is stable. The use of the crystal oscillator provides for a very stable circuit that, when properly tuned, will not give false positives. The maximum range demonstrated by this circuit is approximately 16 inches, which is more than an acceptable range for the intended application. Depending upon the tuning, the target was detected in excess of twenty inches.

A major asset of this particular circuit is that it is field tunable. Tuning can eliminate several real hazards facing mine detection today. The soil is not always uniform. That is to say that it may contain traces of magnetic material that would otherwise cause background noise. The ability to tune this circuit

flexible for application onto several different platforms with different electromagnetic characteristics.

The least squares algorithm seems to produce a good fit for the empirical data. This approach also helps verify some of the gaps in data collection. This empirical formula for inductance is very useful in predicting the inductance of the coil. This is a tremendous help if attempting to tune the circuit to a particular frequency. This allows a calculation that can result in the choice of an appropriate sized capacitor to begin the tuning process. Since the equation from Reference 8 did not apply to the coil used, trial and error was the only method by which to find the correct capacitance for the circuit. This is a very time intensive problem that has been somewhat solved.



## **IV. DISCUSSION**

### **A. APPLICATIONS**

Applications for this project are far reaching. Obviously it would be a tremendous asset to have the technology of autonomous mine detection, classification and destruction. This project is clearly a step in the right direction. The system created here is light weight, portable, relatively inexpensive, and would not increase the cost of the robot significantly. Yet, without a major breakthrough in technology, a metal detecting device is essential to an overall mine sensing system in that many of the other advanced techniques discussed in the introduction have limitations that can only be overcome by sending a metal detector over the area in question, and making a final determination of the object as metal or rock formations. As a part of an intricate sweeping system, this sensor could be used as close as old Fort Ord, and as far away as Korea for cleansing areas of dangerous unexploded ordnance, and land mines.

### **B. FUTURE WORK**

A thesis is currently underway to incorporate a sensor built from the guidelines provided in this thesis with an autonomous mobile robot. Special attention must be paid to the positioning of the sensor on the robot and to the shielding of the sensor from the effects of the of the robot. These effects are

extremely important to understand before sending the robot on a real-time mission.

Other applications are even more intriguing. The problem of identification is not addressed in this thesis. It may be possible to compose a neural network for land mine / unexploded ordnance classification using the results of this thesis. As the system is designed now, a small object located close to the sensor appears to the system exactly the same as a larger object further away. It may be possible to arrange multiple coils in a distinct pattern of geometry, with multiple coil sizes and spacing, so that each size / shape and orientation of a specific object gives off a distinct pattern on each of the coils. This would make the neural network program a relatively simple function of pattern recognition, and would enable a classification to be made.

## LIST OF REFERENCES

1. Steven Ashley, "Searching for Land Mines," *Mechanical Engineering*, Vol. 118/No. 4, April 1996.
2. Jim Lantz, "The Land Mine Dilemma," *The Wall Street Journal*, May 5, 1996.
3. Mark Anglin, "C-MOS Twin Oscillator Forms Micropower Metal Detector," *Electronics* 1977.
4. Pat Cooper, "Counter Mine Technologies Emerge," *Navy Times*, July 22, 1996.
5. Adel S Sedra, Kenneth E. Smith, *Microelectronic Circuits*, third edition, Saunders College Publishing, 1991.
6. "Unexploded Ordnance Advanced Technology Demonstration Program at Jefferson Proving Ground(Phase I)," Report No. SFIM-AEC-ET-CR-94120, U.S. Army Environmental Center, December 1994.
7. William S. Brogan, *Modern Control Theory*, Quantum Publishers, NY, 1974.
8. Robert L. Shrader, *Electronic Communications*, third edition, McGraw-Hill Book Company, NY, 1975.



## INITIAL DISTRIBUTION LIST

1. Defense Technical Information Center.....2  
8725 John J. Kingman Rd., STE 0944  
Ft. Belvoir, VA 22060-6218
2. Dudley Knox Library..... 2  
Naval Postgraduate School  
411 Dyer Rd.  
Monterey, California 93943-5101
3. Chairman, Coded EC.....1  
Department of Electrical and Computer Engineering  
Naval Postgraduate School  
Monterey, CA 93943-5121
4. Dr. D. D. Cleary .....1  
Physics Department, PH/CI  
Naval Postgraduate School  
Monterey, California 93943-5117
5. Dr. Xiaoping Yun.....1  
Department of ECE, EC/Yx  
Naval Postgraduate School  
Monterey, California 93943-5121
6. Curtis Goodnight.....1  
9732 Panama Dr.  
Knoxville TN. 37923